Names and affiliations of applicants (* indicates experimentalists):

Xiao Li, Université catholique de Louvain
Volodia Gounaris, Université catholique de Louvain
Mathieu Vander Donckt, Université catholique de Louvain
Yaroslav Filinchuk, Université catholique de Louvain
Iurii Dovgaliuk, SNBL@ESRF
Vadim Dyadkin, SNBL@ESRF
Dmitry Chernyshov, SNBL@ESRF

Report:

The kinetics of Kr uptake by γ-Mg(BH$_4$)$_2$ was parametrized using two various approaches. The first possibility was based on non-isothermal and isothermal kinetics method. **The non-isothermal kinetics** was analized using variable-temprerature crystallographic Kr occupancies and Kr K-edge fluorescence signal in

Figure 1 – Rietveld refinement and the extracted structural models for the two phases of Mg(BH$_4$)$_2$·nKr at their maximal Kr uptakes. The pores fillings are shown in two projections.
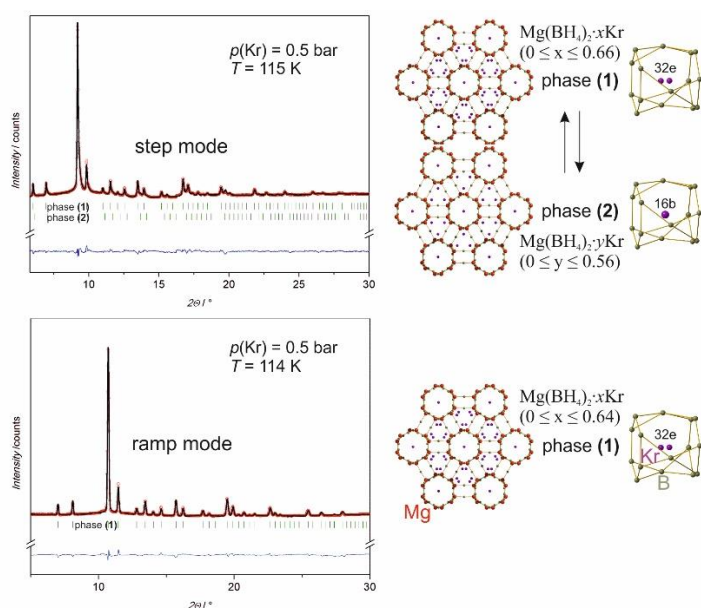
γ-Mg(BH$_4$)$_2$ at fixed cooling and heating rates from 330 to 115 K. The obtained results of non-isothermal data were recently published in [*ACS Appl. Mater. Interfaces* **2020**, 12, 6, 7710-7716]. The main features of this study are related to the proposed two crystal structures of γ-Mg(BH$_4$)$_2$·nKr and the corrresponding mathematical model of their general kinetic uptake. After characterization of the quasi-equilibrium thermodynamics, we turn our attention to non-equilibrium isobars (Figs. 2b, d and e) containing information on adsorption kinetics. We apply an approach based on a first order reaction model. Assuming the Arrhenius kinetics, being a natural choice for an Ising-like lattice model, the temperature dependence of the apparent fraction of the occupied guest sites reads as eq. (1). Here γ_0 is a starting value of the guest occupancy (e. g. 0 on adsorption or a maximal value if we consider the desorption), A is the Arrhenius prefactor, β is the temperature ramp rate, and an integral function in the exponent is given in eq. (2):

$$\alpha(T) = \gamma_{eq}(T) - (\gamma_{eq}(T) - \gamma_0)\exp\left(-\frac{A}{\beta}I(T,T_0,E_a)\right) \quad (1)$$

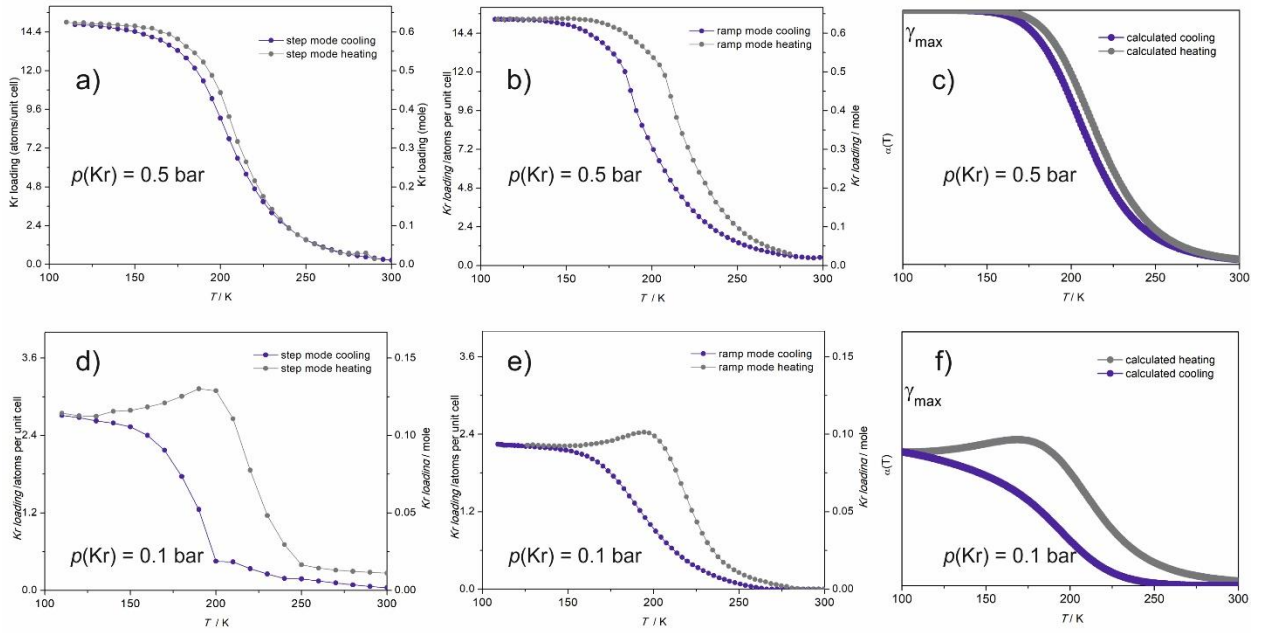$$I(T,T_0,E_a) = \int_{T_0}^{T} e^{-\frac{E_a}{Rx}}dx \quad\quad\quad\quad\quad (2)$$

Figure 2. Temperature-dependent Kr adsorption isobars by γ-Mg(BH$_4$)$_2$ extracted from powder diffraction data collected in the step and ramp modes (a and b for p(Kr) = 0.5 bar, d and e for p(Kr) = 0.1 bar) and the modelled Kr isobars (c and f) from the non-isothermal kinetic model, see equation (2). The contributions from the phases 1 and 2 are shown in Fig. S5.

We found that the estimated activation barrier (10–20 kJ/mol of Kr and the Arrhenius constant A at 0.09–0.2 min^{-1}) from these expctations is of the same order as the activation energies for [BH$_4$]$^-$ reorientations, namely 13.3 to 26.6 kJ/mol in β- and γ-Mg(BH$_4$)$_2$ polymorphs. This hints for a possible correlation of Kr diffusion through pore apertures made of six borohydride groups with reorientational jumps of the [BH$_4$]$^-$ tetrahedra, similar to Li ion diffusion in ht-LiBH$_4$ and some other metal borohydrides. This findings we tried to complement with isothermal kinetic studies, described below.

Isothermal kinetic studies of Kr uptake. We selected the temperatures for kinetic determination, where the Kr sites were filled sligthly higher from the halph of maximally achievable (200, 190, 180 and 170 K, respectively). This temperature interval demonstrates a significant change of the powder pattern's intensities as
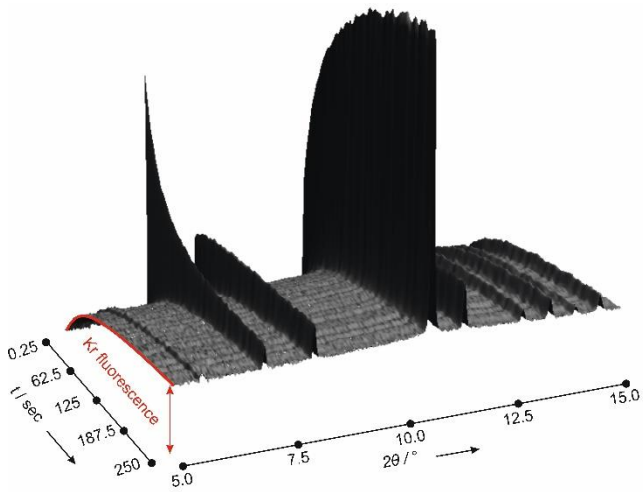

Figure 3. The time-dependent plot of the powder patterns from γ-Mg(BH$_4$)$_2$ loaded with Kr gas (p(Kr) = 0.5 bar, T = 170 K, λ = 0.77936 Å). The significant change in Bragg's intensities and background fluorescence correlate with amount of the adsorbed gas.
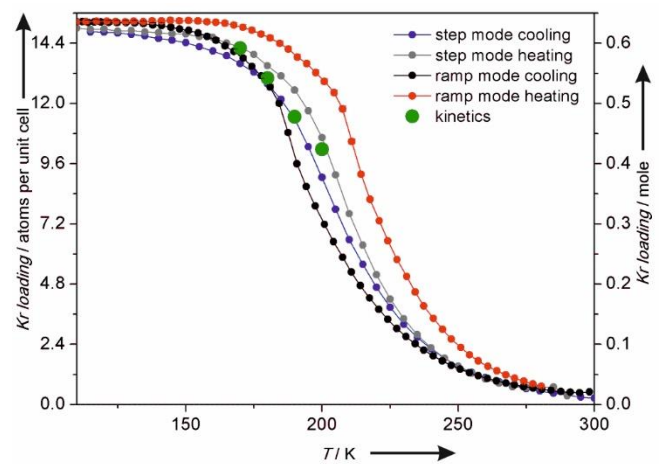
Figure 4. The comparison of calculated Kr content from the isobaric variable-temperature (non-isothermal) experiments and kinetic data. The graph confirms good reproducibility of the step mode variable-temperature data and kinetic maximal (equilibrium) Kr-content.

a function of time upon Kr adsorption by the light γ-Mg(BH$_4$)$_2$ crystal structure, see Fig. 3. The monitoring of the background intensities also confirms highly pronounced increase of Kr fluorescent background in the diffraction patters (Kr fluorescence), which we also used for the monitoring of kinetics of Kr adsorption. The equilibrium (saturation) Kr uptake values are in good agreement with the non-isothermal data, which we demonstarted above, see Fig. 4.

Remarkably, the obtained crystallographic kinetics (Fig. 5) have been fitted assuming two barriers: the first arises due to diffusion through a window and the second along the pore cavities in a porous framework structure:

$$q_t = q_{min} + (q_e - q_{min})[A(1 - \exp(-k_1 t)) + (1 - A)(1 - \exp(-k_2 t))] \qquad (3)$$

Here, q_t is an ammount of Kr adsorbed at time (t, sec), q_e – equilibrium (saturation) Kr content, q_{min} is ammount before the measurment started; $k_{1,2}$ are the kinetic rates and $A < 1$ is a contribution of the adsorbed Kr limited via the first kinetic barrier with a constant k_1. The A is found to be tempearture-dependent, showing the change of the diffusion mechanism domination.
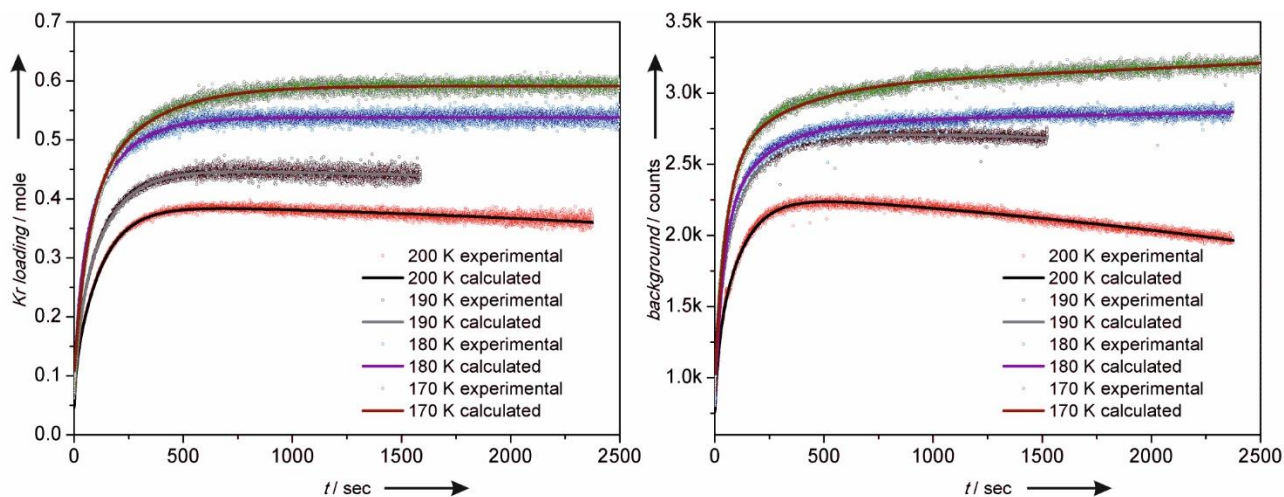

Figure 5. The experimental and calculated curves of the kinetic Kr adsorption (fixed pressure 0.5 bar). The left part corresponds to the Kr occupancies obtained using Rietveld method refinement of the Kr occupancies in phase (1) and (2) and the right part takes into account the fluorescence background.

From the obtained kinetic barriers together with the crystal structure of γ-Mg(BH$_4$)$_2$, we propose two temperature-dependent mechanisms of the kinetics of Kr adsorption: the first is caused via Kr diffusion along 1-D channels in γ-Mg(BH$_4$)$_2$ and it dominates at high temperature (>175 K), while at low temperature (< 175 K) the second mechanism, namely the diffusion through the windows between channels, governs the kinetics. The first kinetic mechanism includes a larger ≈ 5.8 Å aperture of the tubular-like channels, which does not affect the diffusion of Kr (kinetic diameter 3.6 Å) in such an extend as a smaller interchannel aperture with ≈ 5.0 Å size. According to contact surface expectations (0.7 Å grid spacing) made with Mercury, the smaller aperture is adjustable for a diffusion of the guest molecules with a kinetic diameter less than 3.4 Å. Thus, rotation motions of [BH$_4$]$^-$ around 2-fold (C_2) axis of Mg-BH$_4$-Mg bonds with an activation barrier of 13 kJ/mol can favor the diffusion of Kr molecules (kinetic diameter 3.6 Å) via a pedal-wheel mechanism. In such case, the diffusion of larger Xe (4.1 Å kinetic diameter) may be blocked at interchannel aperture and most probably it will be characterized by the first diffusion barrier only. For smaller Ar (kinetic diameter 3.4 Å) the adsorption kinetics should be less sensitive to [BH$_4$]$^-$ rotations as compared with Kr. These results have been submitted to Angewandte Chemie (under review process).

Publications possible thanks to this beamtime allocation (including on spare projects):
1. Dovgaliuk et al., *ACS Appl. Mater. Interfaces* **2020**, 12, 7710-7716.
2. Dovgaliuk et al., *Angew. Chem. Int. Ed.* under revision.
3. Davide Di Stefano, Anna Miglio, Koen Robeyns, Yaroslav Filinchuk, Marine Lechartier, Anatoliy Senyshyn, Hiroyuki Ishida, Stefan Spannenberger, Denise Prutsch, Sarah Lunghammer, Daniel Rettenwander, Martin Wilkening, Bernhard Roling, Yuki Kato, Geoffroy Hautier Superionic diffusion through frustrated energy landscape *Chem.* (Cell press, **impact factor >17**), **2019**, 5, 2450-2460
4. Timothy Steenhaut, Sophie Hermans and Yaroslav Filinchuk, Green synthesis of a large series of bimetallic MIL-100(Fe,M) MOFs, *New J. Chem.*, 2020, Advance Article DOI: 10.1039/D0NJ00257G **with Back Cover**